Supplementary Information

Electrosynthesis-recrystallization method for preparing silver acetate: Application in silver metal-organic decomposition ink

Chenyi Zheng,[a,b,c] Songsong Wang,[a,b,c] Qiang Wang,[b,c,d] Qinmeng Wang,*[a,b,c] and Xueyi Guo*[a,b,c]

(a. School of Metallurgy and Environment, Central South University, Changsha 410083, China;

b. National & Regional Joint Engineering Research Centre of Nonferrous Metal Resources Recycling, Changsha 410083, China;

c. Hunan Key Laboratory of Nonferrous Metal Resources Recycling, Changsha 410083, China

d. School of Chemistry and Chemical Engineering, Central South University, Changsha 410083, China;)

*Corresponding authors:

Qinmeng Wang: qmwang@csu.edu.cn

Xueyi Guo: xyguo@csu.edu.cn

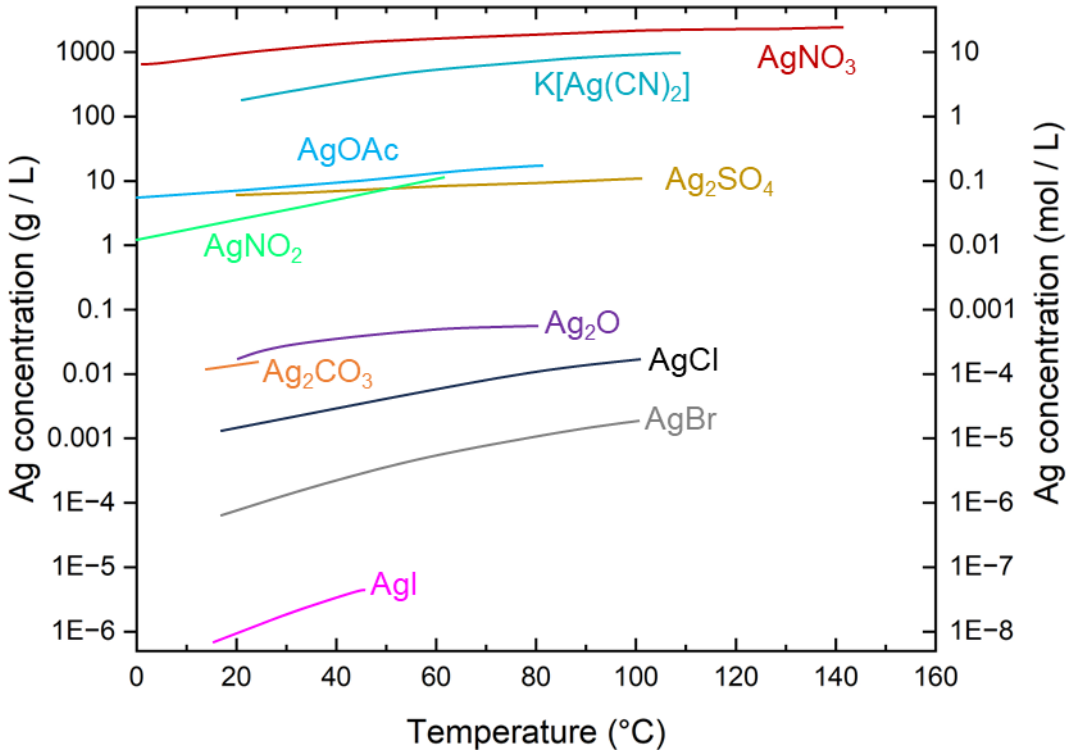

Fig. S1 Solubility of Ag compounds in water.[11]

Supplementary Note 1: Calculation of the Ag^+ enrichment rate in the anolyte (η_{Ag})

The η_{Ag} is estimated according to Eq. (S1), where $w_{Calc.}$ and w_A represent the calculated and measured Ag^+ concentrations (ppm) in anolyte after ES, respectively.

$$\eta_{Ag} = \frac{w_A}{w_{Calc.}} \times 100\% \quad \text{(S1)}$$

The $w_{Calc.}$ is determined by Eq. (S2) based on Faraday's laws.

$$w_{Calc.} = \frac{Q \cdot M_{Ag.} \cdot 10^6}{F \cdot N_A \cdot m_{sol.}} \quad \text{(S2)}$$

Where Q is the charge recorded by the coulombmeter, M_{Ag} is the relative atomic mass of Ag. F is the Faraday constant, N_A is the avogadro constant, and $m_{sol.}$ is the anolyte mass.

The w_A is determined by measuring the Ag^+ concentration in anolyte using ICP-OES, each sample is measured three times, the average value is used.

Table S1 Experimental parameters and analytical results for determining the effect of Ag^+ concentration in anolyte on the η_{Ag}

Exp. #[a]	Temp. (°C)	Current (mA)	Voltage (V)	Duration (h)	Starting and ending pH of catholyte[b]	NaOAc conc. (M)[c]	$w_{Calc.}$ (ppm)[d]	w_A (ppm)[e]	w_C (ppm)[f]	η_A (%)[d]
C-1	25	3.00	3.80	3	3.12 to 3.16	0.1	1811.87	1722.54	1.75	95.07
C-2			3.74	6	3.14 to 3.22		3625.55	3466.75	4.67	95.62
C-3			4.34[g]	9	3.11 to 3.29		5417.33	4506.68	10.49	83.19
C-4			4.70[g]	12	3.07 to 3.39		7206.45	4686.35	19.52	65.03
C-5	50		3.17	3	3.08 to 3.10		1808.14	1730.57	2.69	95.71
C-6			3.09	6	3.12 to 3.23		3600.76	3430.44	5.33	95.27
C-7			3.03	9	3.15 to 3.31		5438.10	5155.86	12.11	94.81
C-8			2.95	12	3.13 to 3.44		7194.45	6807.39	28.71	94.62

[a] Ag and Pt sheets (0.2 × 1.0 × 1.5 cm) served as the anode and cathode, respectively. ES was carried out in an H-type cell whose anodic and cathodic cells each had a volume of 20 mL. The anodic cell was heated with agitation and was sealed to prevent anolyte evaporation. H_2 evolved at the cathode was collected in a gas collection bag.

[b] The pH of the catholyte was adjusted with glacial HOAc prior to the ES process, no further adjustment was made during the ES process. The increase in OAc^- concentration caused by the addition of HOAc is assumed to be small, due to the incomplete ionization of HOAc.

[c] The NaOAc concentration of the anolyte and the catholyte were equal.

[d] Noted in Supplementary Note 1.

[e] Analyzed by ICP-OES, each sample was measured three times, the average value is shown.

[f] w_C represents the Ag^+ concentration in catholyte, which is analyzed by ICP-OES, each sample was measured three times, the average value is shown.

[g] A voltage surge was caused by the crystallization of AgOAc on Ag anode.

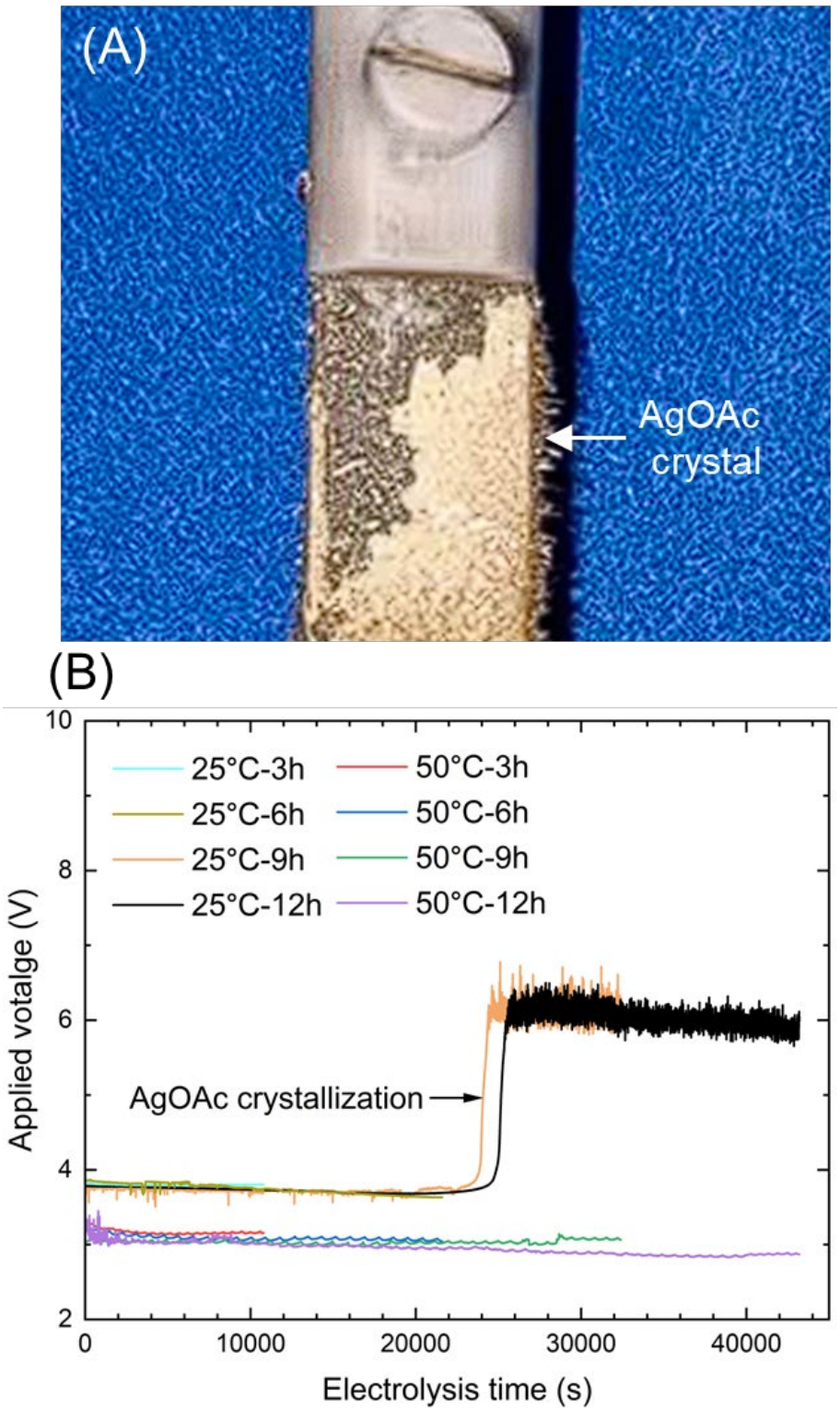

Fig. S2 (A) AgOAc crystallization on Ag anode after #C-4. (B) Galvanostatic curves of #C-1 to 8, #C-1 to #C-4 were carried out at a constant room temperature of 25 °C regulated by air-conditioning. #C-5 to #C-8 were maintained at 50 °C by thermocouple, the corresponding galvanostatic curves exhibit a saw-tooth profile arising from temperature fluctuations.

Table S2 Experimental parameters and analytical results for determining the effect of anolyte temperature on the η_{Ag}

Exp. #[a]	Temp. (°C)	Current (mA)	Voltage (V)	Duration (h)	Starting and ending pH of catholyte[a]	NaOAc conc. (M)[a]	$w_{Calc.}$ (ppm)[b]	w_A (ppm)[a]	w_C (ppm)[a]	η_A (%)[b]
T-1	25	3.00	4.94[c]	12	3.15 to 3.41	0.1	7211.62	4583.71	27.59	63.56
T-2	40		3.68[c]		3.21 to 3.44		7179.36	6282.66	25.18	87.51
T-3	50		2.97		3.11 to 3.41		7180.33	6757.41	33.77	94.11
T-4	60		2.53		3.08 to 3.38		7201.48	6617.44	61.31	91.89
T-5	70		2.26		3.20 to 3.45		7188.11	6191.12	107.33	86.13
T-6	80[d]		2.05		3.19 to 3.47		7175.28	5786.15	144.72	80.64
T-7	90[d]		1.92		3.09 to 3.34		7223.72	5292.82	205.16	73.27

[a] Noted in Table S1.

[b] Noted in Supplementary Note 1.

[c] A voltage surge was caused by the crystallization of AgOAc on Ag anode.

[d] Apparent Ag mirror formation on the anodic cell surface was observed.

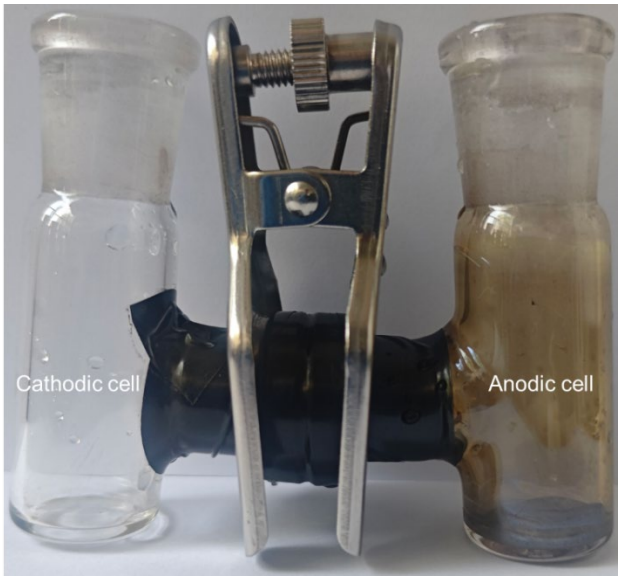

Fig. S3 Ag mirror coated on anodic cell after #T-6.

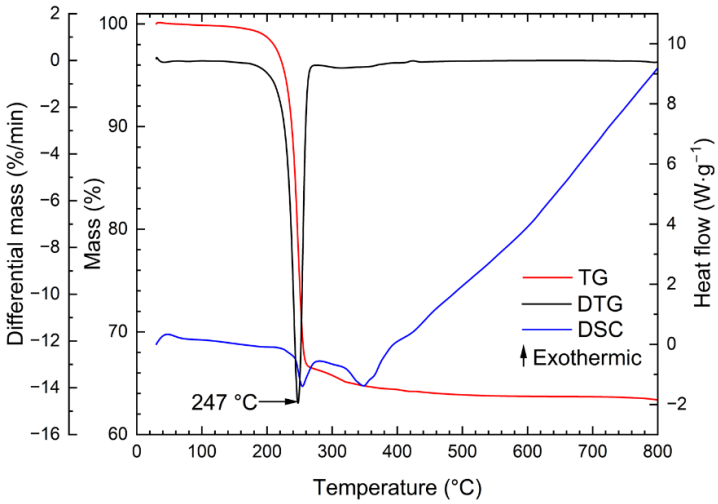

Fig. S4 TG-DSC curve of AgOAc obtained from recrystallization process, heating rate: 10 °C/min.

Table S3 Parameters and results of the thermal decomposition of AgOAc crystals over a prolonged period.

Exp. #[a]	Temperature (°C)	Duration (h)	Mass loss ratio (%)[b]	Insoluble residue (%)[c]
H-1		3	0.13	0.19
H-2		6	0.50	0.83
H-3	90	12	1.83	3.11
H-4		24	9.44	17.84
H-5		48	21.35	37.26

[a] AgOAc crystals obtained from recrystallization process were used.

[b] The mass change before and after heating was determined using an electronic balance.

[c] The heated AgOAc crystal was dissolved in water, and the insoluble residue (metallic Ag) was collected by centrifugation, dried, and weighed to determine the ratio of insoluble residue.

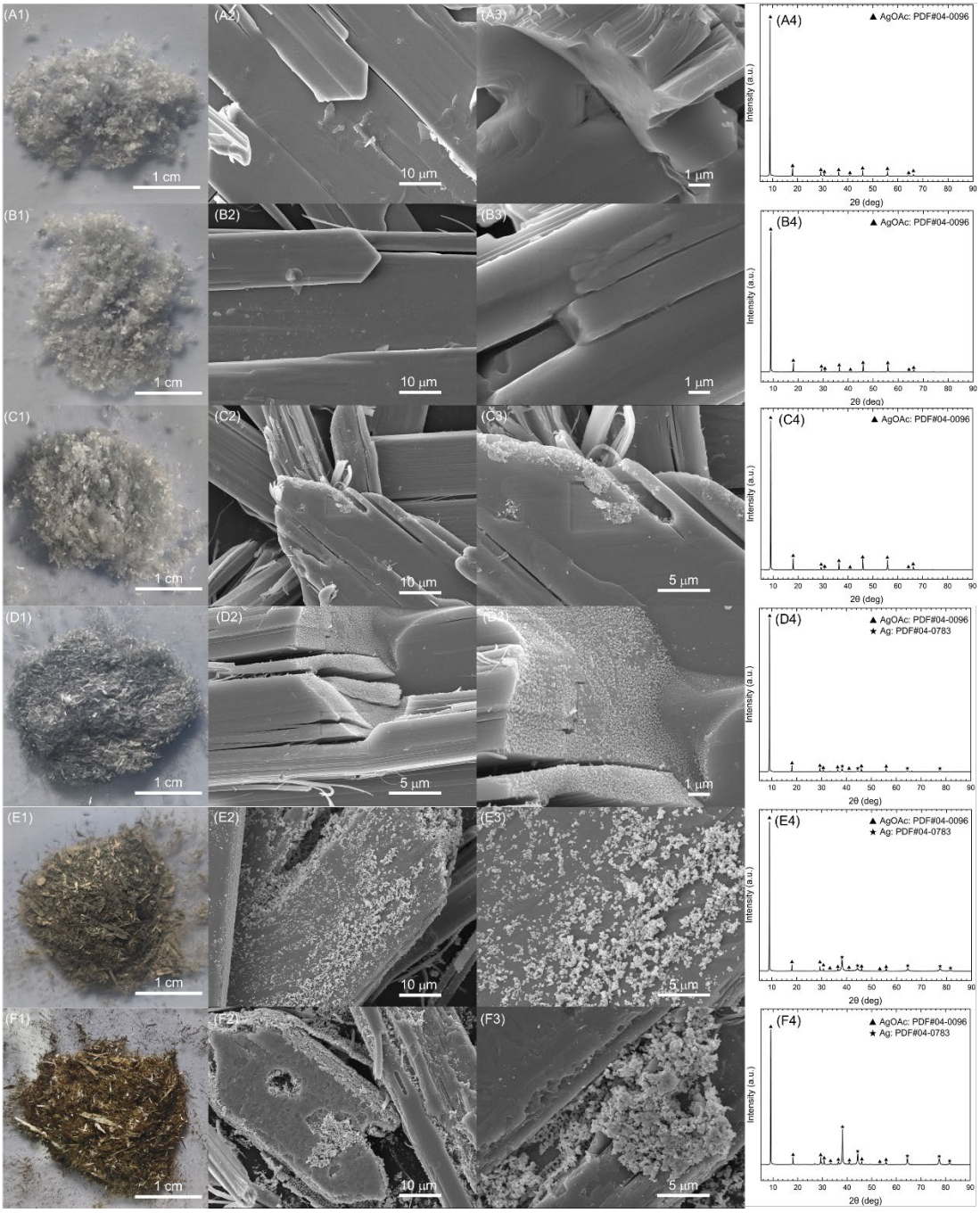

Fig. S5 Changes in AgOAc crystals upon heating at 90 °C for different durations, accompanied by the corresponding SEM images and XRD curves: (A1 to A4) before heating, heating for (B1 to B4) 3 hours, (C1 to C4) 6 hours, (D1 to D4) 12 hours, (E1 to E4) 24 hours, (F1 to F4) 48 hours.

Table S4 Experimental parameters and analytical results for determining the effect of pH on the η_{Ag}

Exp. #[a]	Temp. (°C)	Current (mA)	Average voltage (V)	Duration (h)	Starting and ending pH of catholyte[b]	NaOAc conc. (M)[a]	$w_{Calc.}$ (ppm)[c]	w_A (ppm)[a]	w_C (ppm)[a]	η_A (%)[c]
pH-1	50	3.00	2.93	12	2.74 to 2.97	0.1	7197.44	6793.66	30.48	94.39
pH-2			2.97		3.11 to 3.41		7180.33	6757.41	33.77	94.11
pH-3			3.12		5.92 to 12.03[d]		7205.91	4507.30	NA[e]	62.55
pH-4			3.22		7.98 to 12.41[d]		7221.64	4064.34	NA[e]	56.28
pH-5			3.06		10.87 to 12.94[d]		7187.51	3447.13	NA[e]	47.96

[a] Noted in Table S1.

[b] The pH of the catholyte was adjusted with glacial HOAc and NaOH prior to the ES process, no further adjustment was made during the ES process. The increase in OAc^- concentration caused by the addition of HOAc is assumed to be small, due to the incomplete ionization of HOAc.

[c] Noted in Supplementary Note 1.

[d] Black precipitates were observed in the anodic cell.

[e] Ag^+ precipitates under alkaline conditions and was therefore not analyzed.

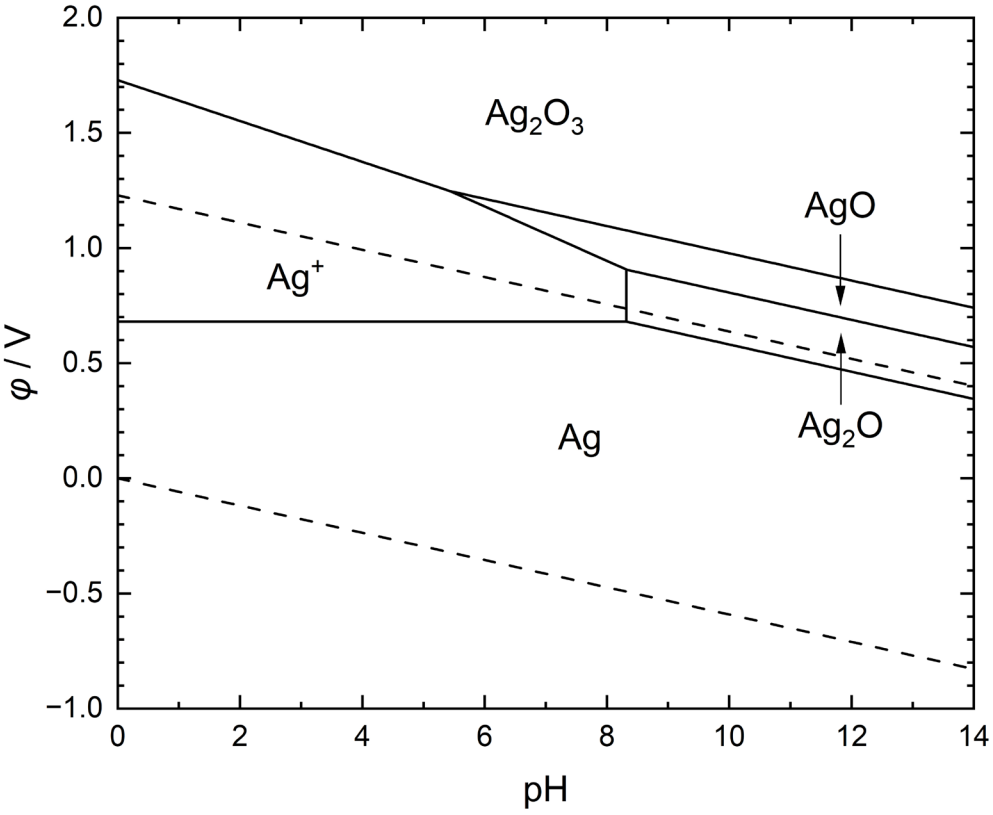

Fig. S6 φ–pH diagram of the Ag–H_2O system with 0.01 M Ag^+ concentration.[23]

Table S5 Experimental parameters and analytical results for determining the effect of applied voltage on the η_{Ag}

Exp. #[a]	Temp. (°C)	Current (mA)	Average voltage (V)	Duration (h)	Starting and ending pH of catholyte[a]	NaOAc conc. (M)[b]	$w_{Calc.}$ (ppm)[c]	w_A (ppm)[a]	w_C (ppm)[a]	η_A (%)[c]
V-1	50	3.00	2.97	12	3.11 to 3.41	0.1	7180.33	6757.41	33.77	94.11
V-2			3.88		3.07 to 3.38	0.07	7172.46	6694.77	36.48	93.34
V-3			5.23		3.20 to 3.40	0.05	7201.13	6571.75	44.22	91.26
V-4			6.91		3.15 to 3.44	0.03	7192.45	6469.61	72.59[d]	89.95
V-5			9.83		3.12 to 3.39	0.01	7223.42	6274.98	88.15[d]	86.87

[a] Noted in Table S1.

[b] By changing the concentration of NaOAc, the voltage during ES can be regulated, the NaOAc concentration of the anolyte and the catholyte were equal.

[c] Noted in Supplementary Note 1.

[d] A substantial electrodeposition of metallic Ag was observed at the cathode.

Table S6 Experimental parameters and analytical results for determining the effect of AEM degradation on the η_{Ag}

Exp. #[a]	Temp. (°C)	Current (mA)	Average voltage (V)	Total duration (h)	Starting and ending pH of catholyte[a]	NaOAc conc. (M)[a]	$w_{Calc.}$ (ppm)[b]	w_A (ppm)[a]	w_C (ppm)[a]	η_A (%)[b]
t-1			3.12	12	3.07 to 3.36		7214.10	6809.39	28.74	94.39
t-2			3.03	24	3.14 to 3.39		7194.66	6785.28	31.54	94.31
t-3			2.96	36	3.03 to 3.29		7185.31	6670.84	30.75	92.84
t-4	50	3.00	3.10	48	3.06 to 3.37	0.1	7203.82	6634.72	44.39	92.10
t-5			2.97	60	3.18 to 3.42		7208.95	6608.44	57.66	91.67
t-6			3.20	72	3.20 to 3.50		7193.36	6506.39	62.88	90.45
t-7			3.09	84	3.09 to 3.33		7159.28	6426.89	74.13	89.77

[a] Noted in Table S1.

[b] Noted in Supplementary Note 1.

Table S7 Experimental parameters and analytical results of the equilibrium experiments for separating AgOAc and NaOAc.

Exp. #[a]	Equilibrium experimental parameters			AgOAc recovery rate (%)[e]	Na/Ag mass ratio[f]
	Mass of the dried crystalline mixture (g)[b]	*L* (mL)[c]	*E* (%)[d]		
E-1	1.15	0.00	100	100	0.41
E-2	1.16	2.51	94.98	99.03	0.098
E-3	1.13	4.99	90.03	97.58	0.014
E-4	1.12	7.48	85.05	96.85	0.0045
E-5	1.15	10.02	79.97	94.56	0.0031
E-6	1.09	12.50	75.01	91.03	0.0015
E-7	1.13	14.99	70.03	89.92	0.0011

[a] 50 mL of the ES anolyte was heated in an evaporating dish (ϕ = 20 cm) at 100 °C until completely dried.

[b] NaOAc exists in both anhydrous and trihydrate forms, the dehydration process is difficult to control during heating, and thus the mass of the dried product exhibits variation. Although prolonged heating can fully dehydrate NaOAc, it also induces thermal decomposition of AgOAc, as shown in Fig. S5.

[c] The volume of deionized water added to the dried crystalline mixture.

[d] Solvent-evaporation rate, calculated according to Eq. (5).

[e] The percentage of recovered AgOAc crystal mass relative to the AgOAc content originally present in the anolyte. AgOAc crystal was collected by filtration using nylon membrane with a pore size of 50 nm, and dried under vacuum at 60 °C.

[f] Analyzed by ICP-OES, each sample was measured three times, the average value is shown.

Table S8 Design and results of response surface analysis for the recrystallization experiments.

Exp. #[a]	*E* (%)[b]	Seed dosage (%)[c]	Cooling rate (°C/min)[d]	stirring intensity (rpm)	AgOAc recovery rate (%)[e]	Na/Ag mass ratio of AgOAc[e]
R-1	84.1	1.5 (0)	1.9 (0)	600 (0)	80.13	0.00073
R-2	85.5	1.5	1.9	600	78.99	0.00074
R-3	86.2	1.5	3.2 (1)	0 (–1)	75.16	0.00061
R-4	83.9	3 (1)	1.9	1200 (1)	83.77	0.00084
R-5	84.4	1.5	1.9	600	80.57	0.00076
R-6	83.8	1.5	0.6	0	66.85	0.00041
R-7	85.4	1.5	3.2	1200	87.52	0.00098
R-8	85.5	0 (–1)	3.2	600	81.62	0.00077
R-9	84.7	1.5	0.6 (–1)	1200	75.41	0.00057
R-10	86.0	3	3.2	600	84.24	0.0009
R-11	85.6	0	1.9	0	68.37	0.00042
R-12	85.2	0	1.9	1200	76.82	0.00058
R-13	84.9	3	1.9	0	70.44	0.00049
R-14	86.2	1.5	1.9	600	81.03	0.00074
R-15	85.4	3	0.6	600	71.42	0.00051
R-16	84.7	1.5	1.9	600	79.56	0.00069
R-17	85.1	0	0.6	600	68.11	0.00039

[a] 50 mL of the ES anolyte was heated in an evaporating dish (ϕ = 20 cm) at 100 °C until the *E* reached approximately 85 %.

[b] The *E* was evaluated by weighing the solution; however, unlike equilibrium experiments, the mass could not be monitored in real time during heating, the *E* exhibited fluctuations.

[c] AgOAc crystal obtained from equilibrium experiments were ground to pass an 800-mesh sieve and employed as the seed, the seed dosage was expressed as a weight percentage of the AgOAc content in the anolyte.

[d] The cooling rate was regulated by varying the cooling method; after the mixture had reached 25 °C, it was kept in a 25 °C water bath for 3 h to allow crystallization.

[e] As noted in Table S7.

[f] The room temperature was maintained at 20 °C by air conditioning; after 46.7 min of cooling to 25 °C.

[g] The mixture was cooled in a refrigerated cup held at 6 °C and reached 25 °C within 23.3 min.

[h] The mixture was cooled sequentially in water baths at 70 °C and 40 °C, and finally in air at 20 °C, reaching 25 °C after 124.3 min.

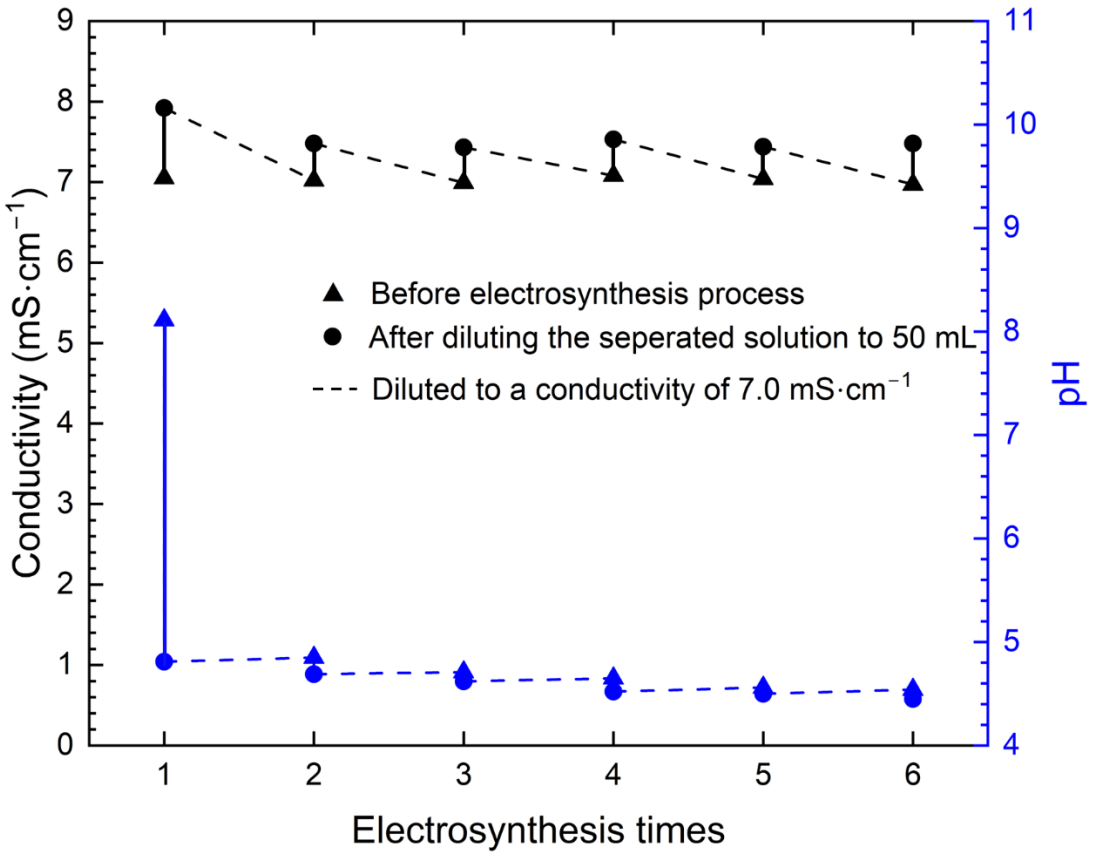

Fig. S7 Variations in conductivity and pH of the NaOAc solutions during repeated recycling.

Supplementary Note 2: Economic and environmental benefit of ES-R method in AgOAc production

Owing to the lack of life cycle assessment data for the industrial production of $AgNO_3$, and the ES-R method has not yet been scaled up to pilot scale, the discussion can currently only be conducted based on a comparison of laboratory-scale data. The discussion can be carried out from the following aspects.

(1) Power consumption of ES-R method:

The power consumption of the ES process was calculated based on typical laboratory cases (Table S1~S6). The applied voltage of the ES process was assumed to be 3 V, and the theoretical AgOAc yield was calculated according to Faraday's Law. Assuming that the η_A was set at 94% and the recovery rate of AgOAc after recrystallization was set at 96%, and adopting the electricity price of ~0.1 USD per kilowatt-hour in compliance with China's electricity tariff standards, the electricity cost for producing 1 ton of AgOAc was determined to be 74.42 USD.

(2) Cost savings compared with the nitrate synthesis route:

①Since the intermediate product of $AgNO_3$ is no longer required, the consumption of H_2O_2 during the $AgNO_3$ preparation is avoided. The dosage of H_2O_2 can be calculated according Eq. (1)[13].

$$2Ag + 2HNO_3 + H_2O_2 \rightarrow 2AgNO_3 + 2H_2O \quad (1)$$

Based on the price of industrial H_2O_2 with a concentration of 30%, it can be calculated that a cost reduction of 116.34 USD in H_2O_2 is achieved during the production of 1 ton of AgOAc.

②Similarly, since it is no longer necessary to use Na_2CO_3 for the preparation of Ag_2CO_3 as the intermediate product (Eq. (2 and 3)), the cost of Na_2CO_3 can be reduced, and the CO_2 emissions can also be mitigated simultaneously[12,15].

$$2AgNO_3 + Na_2CO_3 \rightarrow Ag_2CO_3 + NaNO_3 \quad (2)$$

$$2HOAc + Ag_2CO_3 \rightarrow 2AgOAc + H_2O + CO_2 \quad (3)$$

Based on the price of industrial Na_2CO_3, it can be calculated that a cost reduction of 59.04 USD in Na_2CO_3 is achieved during the production of 1 ton of AgOAc, with a simultaneous reduction of 131.81 kg in CO_2 emissions.

③Furthermore, since nitrate wastewater is no longer generated, the corresponding treatment costs can also be saved. However, as the treatment methods vary with the concentrations of nitrate wastewater, it is difficult to standardize the associated costs, the exact amount of savings cannot be calculated.

(3) Potential benefits from by-products:

Green H_2 is generated as a by-product during the ES process. If it can be collected and sold, an additional revenue of 25.96 USD can be obtained for the production of 1 ton of AgOAc, based on the industrial price of green H_2.

(4) Streamline the production process to enhance efficiency:

The industrial production of $AgNO_3$ involves multiple steps[14], and the resulting $AgNO_3$ still requires replacement and acid dissolution reactions to produce AgOAc. This low-efficiency production method has limited the application of AgOAc in the MODI field. The overall reaction equation of the ES-R method is shown in Eq. (6), which effectively improves the production efficiency.

$$Ag + HOAc \rightarrow AgOAc + \frac{1}{2}H_2 \quad (6)$$

Table S9 Experimental parameters and analytical results for determining the effect of AgOAc content on the ρ.

Exp. #	Ag MODI chemical composition (%)			Curing parameter	ρ (μΩ·cm)[c]
	Organic vehicle[a]	Adhesive[b]	AgOAc		
MODI-1	80.2	15.0	4.8	110 °C for 3h	10948.6
MODI-2	74.8		10.2		1257.2
MODI-3	69.4		15.6		401.5
MODI-4	64.1		20.9		42.3
MODI-5	59.6		25.4		37.1
MODI-6	54.0		31.0		29.7

[a] A mixture of IPA, deionized water, and formic acid is prepared at a mass ratio of 18:8:3.

[b] 3% HEC aqueous solution serves as the adhesive.

[c] Calculated according to Eq. (7).

Table S10 Summary of reported studies on Ag MODI.

Precursor	Decomposition temp./time (°C/min)	Resistivity (μΩ·cm)	Ag content (%)	References
Silver acetate	(microwave plasma)/1.5	7.14	22.44	[28]
Silver oxalate	130/30	25.1	24.7	[30]
Silver oxalate	200/10	3.5	27.6	[31]
Silver itaconate	≤70 (plasma)/60	5.26	14.4	[32]
Silver acetate and silver oxide	160/40	7.2	15-20	[33]
Silver acetate	110/180	42.3	13.5	This study

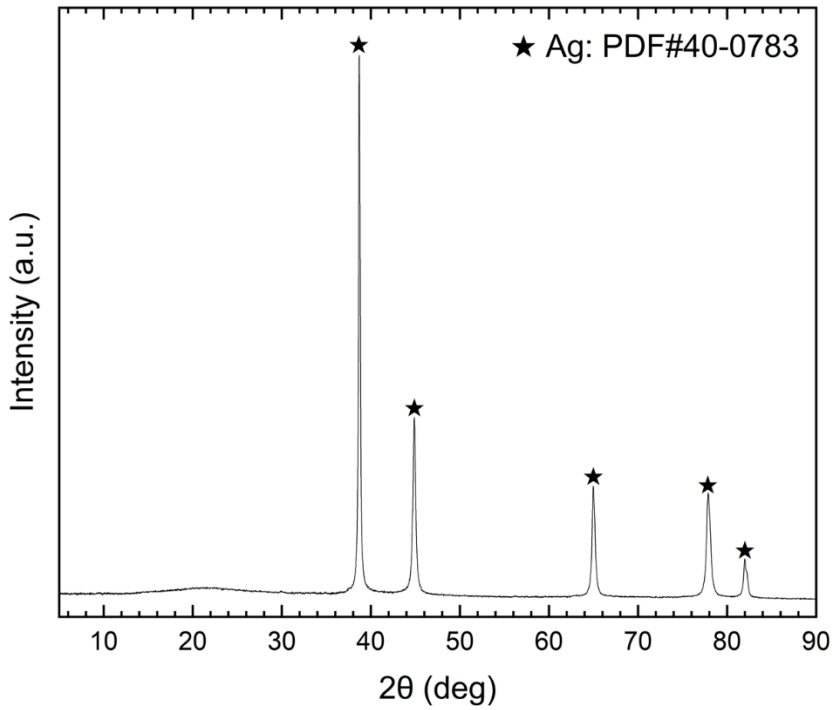

Fig. S8 XRD curve of the cured Ag MODI conductive pattern on glass substrate, scan rate: 5° / min.

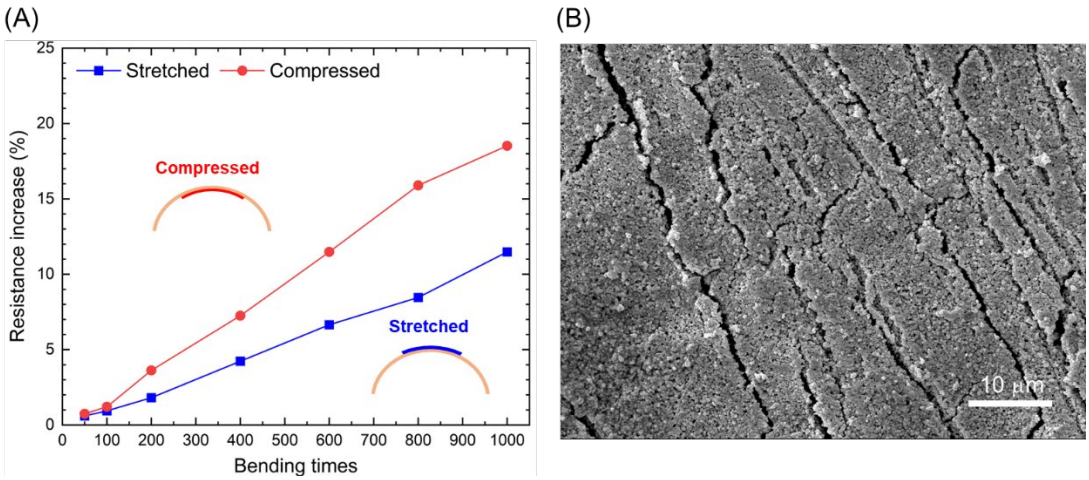

Fig. S9 (A) Resistance change of MODI pattern during the bending test, (B) SEM image of the MODI pattern after bending test.

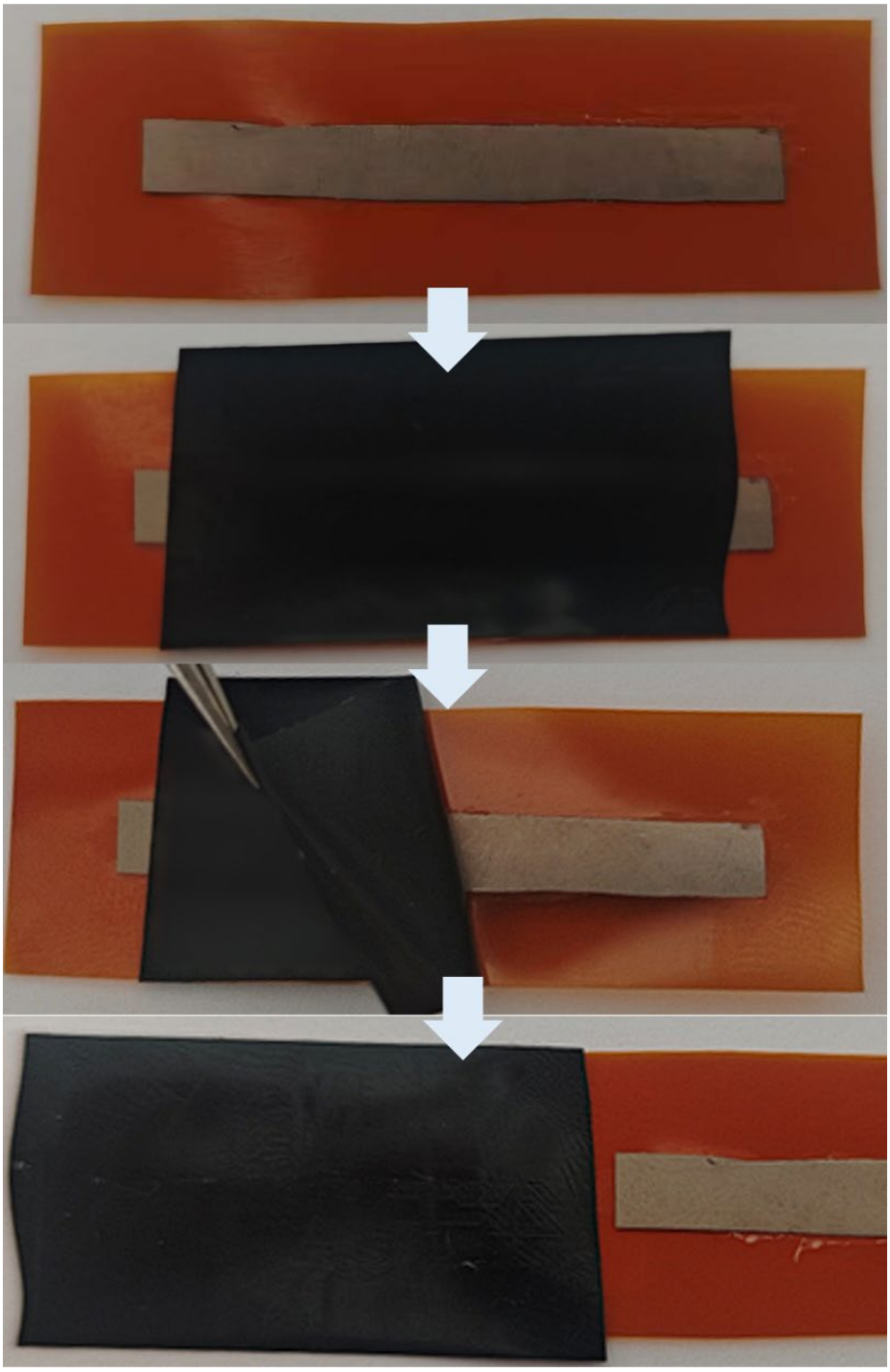

Fig. S10 Tape peel-off test for assess the adhesion between the Ag layer and the substrate.